Contribution from the Chemistry Department,
Brookhaven National Laboratory, Upton, New York 11973

Kinetics of Ferrate(V) Decay in Aqueous Solution. A Pulse-Radiolysis Study

J. D. Rush[†] and Benon H. J. Bielski*

The kinetic and spectral properties of pentavalent iron derived from pulse-radiolytic reduction of aqueous ferrate(VI) by 2-propanol radicals have been characterized over the pH range 6.3–13. Three forms of iron(V) occur over this pH range, which are represented by the following equilibria: $H_2FeO_4^- \rightleftharpoons H^+ + HFeO_4^{2-}$, $pK_2 = 7.5$; $HFeO_4^{2-} \rightleftharpoons H^+ + FeO_4^{3-}$, $pK_3 = 10.1$. The protonated forms of ferrate(V) are unstable due to decomposition by a second-order process that results in the formation of hydrogen peroxide and ferric ions rather than disproportionation. The bimolecular rate constants in 1 mM phosphate/borate buffer at 25 °C are $k_1(H_2FeO_4^- + H_2FeO_4^-) = (9 \pm 2) \times 10^7$ M^{-1} s^{-1}, $k_2(H_2FeO_4^- + HFeO_4^{2-}) \approx 3 \times 10^7$ M^{-1} s^{-1}, $k_3(HFeO_4^{2-} + HFeO_4^{2-}) \approx 1.5 \times 10^7$ M^{-1} s^{-1}, and $k_4(HFeO_4^{2-} + FeO_4^{3-}) = (1.0 \pm 0.2) \times 10^7$ M^{-1} s^{-1}. At higher pH, FeO_4^{3-} decays by a unimolecular process, $k_f = 8 \pm 1$ s^{-1}. The very high second-order rates as well as the peroxide product suggest that oxide ligands bound to ferrate(V) may have a much higher degree of free-radical character than does the parent ferrate(VI) ion.

Introduction

The aqueous chemistry of hypervalent iron is usually not accessible to commonly used techniques, and therefore not much is known about the reactivity of iron species in oxidation states higher than III. An exception to this is the ferrate(VI) ion, which is a well-characterized species as regards structure,[1] spectral properties,[2,3] and, to an extent, chemical reactions[4a–d] that are not atypical of the high-valent metallo–oxo anion species for the first-row transition metals. The oxygen–iron bonds in ferrate(VI) are equivalent, and Mössbauer spectroscopy[5] indicates a high degree of covalent character. This accounts for the slow rate at which the oxide ligands exchange with solvent water.[6] A very characteristic feature of the ferrate(VI) ion is the manner in which it decays to iron(III) and O_2 in solution,[3] which is predominantly second order and strongly pH dependent. An extensive study of these processes[7] has identified two protonated forms that are particularly reactive, and only the fully deprotonated FeO_4^{2-} is relatively stable in alkaline solution.

We have been interested in ferrate(IV) and ferrate(V), oxidation states that are frequently postulated as kinetic transients in ferrate(VI) decay,[7,8] the action of catalases and peroxidases,[9] and iron-catalyzed organic hydroxylation reactions.[10,11] Although the organic environment of iron may considerably modify its properties, the activation of oxygen or peroxide by formation of a ferryl (Fe=O^{2+}) or perferryl (Fe=O^{3+}) system is thought to be an important feature of many biochemical mechanisms involving iron-containing enzymes.[9] Previous investigations by pulse radiolysis[12,13] of the simplest forms of these species, obtained by the free-radical oxidation or reduction of ferric or ferrate(VI), respectively, yielded spectral data and showed that these are short-lived species. In 4 M NaOH ferrate(V) decays at a rate of 4 s^{-1}. In the present study we have examined the spectral and kinetic properties of ferrate(V) decay between pH 6 and 13 in order to obtain closer comparisons with the parent ferrate(VI) ion and to obtain additional information on the factors contributing to the reactivity of the oxo–iron bond.

Experimental Section

All solutions were prepared by using water that, after distillation, had been passed through a Millipore ultrapurification system. Common chemicals were of reagent grade or better purity. Phosphate or phosphate/borate buffers of 1 mM total concentration were used in most experiments. Salts of $NaClO_4$ and $LiClO_4$, used in ionic strength effect studies, were twice recrystallized, once from Milli-Q water containing 20 μM DTPA and once from Milli-Q water alone. The nitrous oxide used as a saturating and blanket gas was of 99.99% purity (UHP grade, Matheson).

Potassium ferrate (K_2FeO_4) of high purity was prepared as previously described.[13,14] Its solutions ($1.0–1.8 \times 10^{-4}$ M) are stable at pH >8 and are relatively unreactive toward alcohols at the low ($2–3 \times 10^{-3}$ M) concentrations used in the experiments. A molar absorptivity of 1150 M^{-1} cm^{-1} at 510 nm (at pH 9 or above)[13] was used to calculate fer-
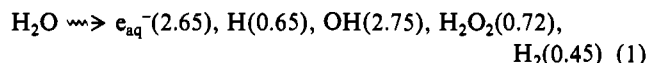
rate(VI) concentrations. For experiments below pH 8, where ferrate(VI) is unstable, the ferrate(VI) solutions were premixed to the desired pH with a phosphate buffer in a jet-mixing apparatus and pulsed within 10 s.

Pulse-radiolysis experiments were carried out with the BNL 2-Me Van de Graaff accelerator according to procedures described elsewhere.[15] Doses were computed by the KSCN dosimeter, assuming $G[(SCN)_2^-] = 6.13$. Kinetic analyses were performed by nonlinear least-squares fits to the traces by first- or second-order routines. Observed second-order rate constants were calculated from linear plots of the rate constants against dose, which typically was varied to produce initial Fe^V concentrations $(3–15) \times 10^{-6}$ M.

Steady-state radiolysis was performed in a ^{60}Co γ-ray source (≈600 rad/min), which was previously calibrated with a Fricke dosimeter. N_2O-saturated solutions of pH 10 containing $1.2–1.5 \times 10^{-4}$ M ferrate, 5×10^{-3} M 2-propanol, and 5×10^{-4} M EDTA were irradiated for 30-s intervals, and the decrease in optical density at the 510-nm maximum of ferrate(VI) was measured against a nonirradiated blank. Similar conditions were also employed in experiments containing in addition 0.2, 1.3, and 2.6 μM bovine liver catalase (Sigma) to prevent accumulation of H_2O_2. From the dose rate it was calculated that the isopropyl radical was generated at a rate of 6.7×10^{-6} M/min.

Results and Discussions

Reduction of Fe(VI) to Fe(V). The radiolysis of water yields the following radicals and molecules:

$$H_2O \rightsquigarrow e_{aq}^-(2.65), H(0.65), OH(2.75), H_2O_2(0.72),$$
$$H_2(0.45) \quad (1)$$

where the values in parentheses are G values, that is, the number

Table I. Second-Order Rate Constants for the Reduction of Permanganate(VII) and Ferrate(VI) by 2-Propanol and Ethanol Radicals at pH 10.4, 25 °C

	$10^{-9}k((CH_3)_2\dot{C}OH)$	$10^{-9}k(CH_3\dot{C}HOH)$
Mn^{VII}	7.2 ± 1	3.3 ± 0.5
Fe^{VI}	3.0 ± 1	8.0 ± 1.5

(1) Hoppe, M. L.; Schlemper, E. L.; Murmann, R. K. *Acta Crystallogr., Sect B* **1982**, *B38*, 2237.
(2) Carrington, C.; Schonland, D.; Symons, M. C. R. *J. Chem. Soc.* **1957**, 659.
(3) Wood, R. H. *J. Am. Chem. Soc.* **1958**, *80*, 2038.
(4) (a) Williams, D. H.; Riley, J. T. *Inorg. Chim. Acta* **1974**, *8*, 177. (b) Carr, J. D.; Kelter, P. B.; Ericson, A. T. *Environ. Sci. Technol.* **1981**, *15*, 184. (c) Audette, R. J.; Quail, J. W.; Smith, P. J. *J. Chem. Soc., Chem. Commun.* **1972**, 38. (d) Groves, J. T.; McClusky, G. A. *J. Am. Chem. Soc.* **1976**, *98*, 859.
(5) Heber, R. H.; Johnson, D. *Inorg. Chem.* **1979**, *18*, 2786.
(6) Goff, H.; Murmann, R. K. *J. Am. Chem. Soc.* **1971**, *93*, 6058.
(7) Carr, J. D.; Kelter, P. B.; Tabatabai, A.; Spichal, D.; Erickson, J.; McLaughlin, C. W. *Proc. Conf. Water Chlorination Chem. Environ. Impact Health Effects,* 1985.
(8) Kalecinski, J. *Rocz. Chem.* **1967**, *41*, 661.
(9) Groves, J. T. *Metal Ion Activation of Dioxygen*; Spiro, T. G., Ed.; Wiley: New York, 1980; pp 125–162 and references therein.
(10) Rush, J. D.; Koppenol, W. H. *J. Am. Chem. Soc.* **1988**, *110*, 4857.
(11) Sugimoto, H.; Sawyer, D. T. *J. Am. Chem. Soc.* **1984**, *106*, 4283.
(12) Rush, J. D.; Bielski, B. H. J. *J. Am. Chem. Soc.* **1986**, *108*, 523.
(13) Bielski, B. H. J.; Thomas, M. J. *J. Am. Chem. Soc.* **1987**, *109*, 7761.
(14) Thompson, G. W.; Ockerman, L. T.; Schreyer, J. M. *J. Am. Chem. Soc.* **1951**, *73*, 1379.
(15) Rush, J. D.; Bielski, B. H. J. *J. Phys. Chem.* **1985**, *89*, 5062.

†Present address: Department of Chemistry, Louisiana State University, Baton Rouge, LA 70803-1804.
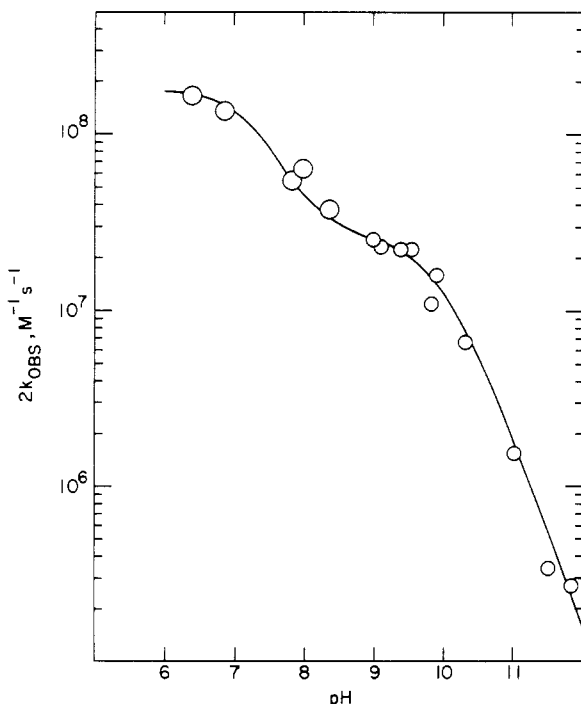
Figure 1. Observed rate constants for the bimolecular decay of ferrate(V) in 1 mM phosphate/borate buffer at 25 °C. The solid curve is fitted by using eq 4–6 with the parameters given in Table III.

of radicals or molecules formed per 100 eV of energy dissipated in water.[16] The primary radicals react with additives: in the present studies the solutions were saturated with N_2O and contained either ethanol or 2-propanol. Above pH 9.6[16] the H atoms are converted to hydrated electrons, which react with nitrous oxide to form hydroxyl radicals ($e_{aq}^- + N_2O + H_2O \rightarrow OH + OH^- + N_2$).[17] The OH radicals react with alcohols via hydrogen abstraction predominantly at the α-carbon position, yielding a reducing carbon-centered radical according to eq 2.[18] Other radicals

$$OH + (CH_3)_2CHOH \rightarrow H_2O + (CH_3)_2\dot{C}OH \qquad (2)$$
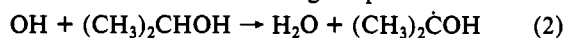
are formed in minor yields, and most are converted to the α-carbon-centered form. The G value of reducing radicals in eq 3

$$(CH_3)_2\dot{C}OH + ferrate(VI) \rightarrow (CH_3)_2CO + ferrate(V) \qquad (3)$$

was checked against the yield of manganate(VI) formed in the reaction of alcohol radicals with permanganate(VII) by using the well-established molar absorptivities of these species[19] and was found to be 6.1 ± 0.1. Comparative second-order rate constants measured for the reduction of Mn(VII) and Fe(VI) by these alcohol radicals are given in Table I.

Kinetics of Ferrate(V) Decay. Ferrate(V) decays by mixed second-order and first-order pathways. The first-order rate is relatively important only at pH's greater than about 11 and can be measured from the intercept of the dose dependence of second-order observed rates, while in 0.1 M NaOH (pH 13) it is effectively the only path. At lower pH's, the second-order process is so much faster than the first-order decay rate that the latter cannot be reliably measured. The variation of the second-order rate of disappearance of ferrate(V) with pH is shown in Figure 1. The kinetic fit is obtained by postulating two pK_a's of the ferrate(V) ion in the pH range studied (6.3–13), where $pK_2 = 7.5$ and $pK_3 = 10.1$ correspond to the equilibria
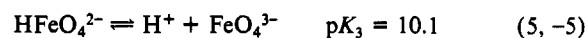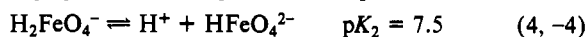
$$H_2FeO_4^- \rightleftharpoons H^+ + HFeO_4^{2-} \qquad pK_2 = 7.5 \qquad (4, -4)$$

$$HFeO_4^{2-} \rightleftharpoons H^+ + FeO_4^{3-} \qquad pK_3 = 10.1 \qquad (5, -5)$$

Table II. Dependence of k_f on Ferrate(VI) Concentration at pH 11.5 in 5 mM Phosphate and $[Fe^V]_0 = 3.0~\mu M$ at 25 °C

[ferrate(VI)], M	k_f, s^{-1}	[ferrate(VI)], M	k_f, s^{-1}
1.2×10^{-5}	8 ± 0.5	6.2×10^{-4}	13 ± 1.0
2.6×10^{-4}	11 ± 1.0		

Table III. Kinetic Fitting Parameters Determined in 1 mM Phosphate/Borate at 25 °C

$k_1 = (9 \pm 2) \times 10^7~M^{-1}~s^{-1}$	$k_4 = (1.0 \pm 0.2) \times 10^7~M^{-1}~s^{-1}$
$k_2 \sim 3 \times 10^7~M^{-1}~s^{-1}$	$k_5 = (8 \pm 1)~s^{-1a}$
$k_3 \sim 1.5 \times 10^7~M^{-1}~s^{-1}$	

^{a}Determined at pH 10.35, 11.0, 11.5, and 13.
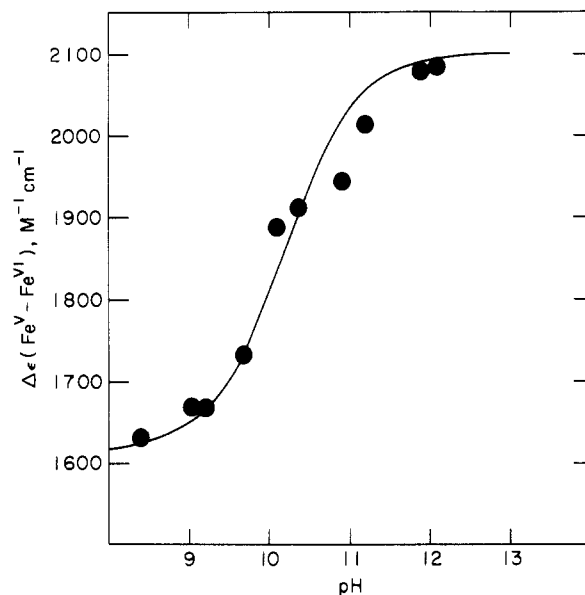

Figure 2. Dependence of the ferrate(V) spectrum on pH. The increase in ϵ at 270 nm on reducing ferrate(VI) to ferrate(V) with 2-propanol radicals is plotted against pH, showing a $pK_a(HFeO_4^{2-} \rightleftharpoons FeO_4^{3-} + H^+) = 10.1$ with a curve fitted to this value.

An additional deprotonation most likely occurs at pH <6.0, well below the present experimentally accessible range. The overall rate law for ferrate(V) decomposition at low concentrations of ferrate(VI) is described by eq 6, where the experimental values

$$-d[Fe(V)]/dt = 2k_{obs}[Fe(V)]^2 + k_f[Fe(V)] \qquad (6)$$

of k_{obs} are dependent on the ferrate(V) species present. A very minor pathway is also observed when ferrate(VI) is varied from 1.2×10^{-5} to 6×10^{-4} M, which causes an increase in the measured first-order decay component, k_f (Table II). This apparent interaction between ferrate(V) and ferrate(VI) is usually insignificant in pulse-radiolysis experiments, but it appears to have an effect during steady-state radiolysis. The observed second-order decay rates are the sum of four separate reactions (rate constants k_1-k_4) between ferrate(V) species:

$$k_{obs}[Fe^V]^2 = k_1[H_2FeO_4^-]^2 + k_2[H_2FeO_4^-][HFeO_4^{2-}] +$$
$$k_3[HFeO_4^{2-}]^2 + k_4[HFeO_4^{2-}][FeO_4^{3-}] \qquad (7)$$

The rate constants were evaluated by fitting the experimental data and are listed with approximate uncertainties in Table III. The rate constants k_2 and k_3, whose values are strongly interdependent, are listed as estimated values. The equilibrium constant K_3 was independently evaluated from the pH dependence of the ferrate(V) spectrum at 270 nm, where the species that are probably the doubly and triply deprotonated forms have a maximum difference in absorbance. These data are plotted in Figure 2, and individual molar absorptivities in the UV range are given in Table IV. The pK_2 of ferrate(V) could not be independently measured in this fashion, since the parent ferrate(VI) spectrum is strongly pH dependent in this pH range ($pK_a(HFeO_4^-/FeO_4^{2-}) = 7.8$).[7] However, the ferrate(V) spectrum measured at pH 6.3 is different

(16) Schwarz, H. A. *J. Chem. Educ.* **1981**, *58*, 101.
(17) Schuler, R. H.; Patterson, L. K.; Janata, E. *J. Phys. Chem.* **1980**, *84*, 2089.
(18) Willson, R. L.; Greenstock, C. L.; Adams, G. E.; Wageman, R.; Dorfman, L. M. *Int. J. Radiat. Phys. Chem.* **1971**, *3*, 211.
(19) Fielden, E. M.; Hart, E. J. *Radiat. Res.* **1967**, *32*, 564.

Table IV. Extinction Coefficients in the Ultraviolet Range for $HFeO_4^{2-}$ and FeO_4^{3-}

wavelength, nm	$\epsilon(HFeO_4^{2-})$,[a] 10^{-3} M^{-1} cm^{-1}	$\epsilon(FeO_4^{3-})$,[b] 10^{-3} M^{-1} cm^{-1}
250	5.3	5.7
260	5.2	5.6
270	4.7	5.3
280	4.5	4.8
290	4.0	4.3
300	3.45	3.8
310	2.9	3.1
320	1.8	1.9
330	1.2	1.25
340	0.93	1.05

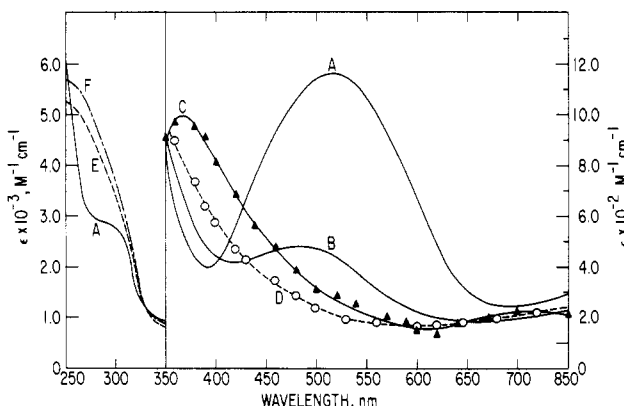[a] Measured at pH 9.0. [b] Measured at pH 11.2. [c] ϵ's are within ±5% error.

Figure 3. UV/visible absorption spectra of ferrate(V) and ferrate(VI) ions: (A) FeO_4^{2-}, pH >9.0 (solid line taken from ref 13); (B) $HFeO_4^-$, pH 6.3 (shown for comparison with Fe^V); (C) $HFeO_4^{2-}$, pH 9.0 (▲, visible range); (D) $H_2FeO_4^-$, pH 6.3 (O, visible range); (E) $HFeO_4^{2-}$, pH 9.0 (---, UV range; see Table IV); (F) FeO_4^{3-}, pH 11.2 (— — — UV range; see Table IV).

from that obtained at pH 9 and accords with the kinetically measured pK_2. The absorption spectra in the range 350–700 nm for the ferrate(V) species $H_2FeO_4^-$, $HFeO_4^{2-}$, and the mono-protonated ferrate(VI), $HFeO_4^-$, are shown in Figure 3. The last spectrum was obtained by pH jump of alkaline ferrate(VI) solutions to pH 6.3 and was used as a reference for calculating the spectrum of $H_2FeO_4^-$. The significant decrease in the large peak at 510 nm is consistent with a previous study of spectral changes occurring upon protonation.[7] The visible spectrum of mono-protonated ferrate(V) is virtually indistinguishable from that of the deprotonated form.[12,13]

The spectra, mode of decay (mixed unimolecular and bimolecular processes), and pH dependences suggest that ferrate(V) and ferrate(VI) are analogous species with respect to their structure. The broad absorbance at wavelengths greater than 600 nm is virtually unchanged in both oxidation states regardless of pH, which suggests a common tetrahedral oxyanion structure. Ferrate(VI) has pK_a's of 3.5 and 7.8[7] whereas ferrate(V), within the experimentally accessible pH range, has pK_a's at 7.5 and 10.1. The first pK_a of H_3FeO_4 might occur at about pH 3–4, which would be compatible with the range of acidity constants exhibited by various pentavalent oxyanions.

An attempt was made to verify the charge assignment by measuring the ionic strength dependence of Fe(V) decay though the reactions are complex and the Debye–Huckel limiting law is not always reliable in the range 0.01 M $\leq \mu \leq$ 0.2 M. It was found that k_{obs} not only increases with ionic strength (see Table V) but is dependent upon the electrolyte cation. In 0.1 M LiClO₄ k_{obs} is about half of what it is in 0.1 M NaClO₄, which is likely due to the greater affinity of the small lithium cation for a species such as FeO_4^{3-}. It also seems likely that such ion pairing lowers the proton affinity of FeO_4^{3-} and hence the overall rate of Fe(V) decay. The bimolecular rate constants given in Table III are not corrected for electrostatic factors though ion pairing at the ex-

Table V. Ionic Strength Dependence of the Bimolecular Rate of Ferrate(V) Decay at pH 9.0 in 2 mM Borate Buffer + NaClO₄ at 25 °C

ionic strength, M	$10^{-7}k_{obs}$, M^{-1} s^{-1}	ionic strength, M	$10^{-7}k_{obs}$, M^{-1} s^{-1}
0.011	1.00	0.20	2.00
0.021	1.15	0.11 (LiClO₄)	0.90
0.10	1.75		

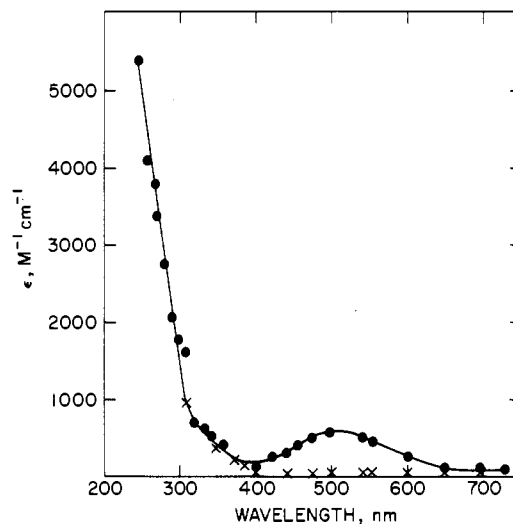**Figure 4.** Spectrum of the initial product of ferrate(V) decay observed at pH 9 or above (●). At pH 6.3, the absorbance peak at 500 nm is not observed (×).

perimental concentrations of Na^+ (2–3 mM) is probably not extensive. If the Debye–Huckel theory is used to correct for electrostatic factors, k_4 is expected to be nearly 10^9 M^{-1} s^{-1} at μ = 1 M (i.e. about 10% of the diffusion-controlled rate constant for uncharged species), while k_1–k_3 all exceed 3 × 10^8 M^{-1} s^{-1}.

Products of Ferrate(V) Decomposition. When ferrate(V) decomposition by either first- or second-order pathways is complete, a residual spectrum with strong UV absorbance and a broad peak at 500 nm ($\epsilon \approx$ 550 M^{-1} cm^{-1}) is observed at pH's greater than about 9. At pH 6.3 disappearance of ferrate(V) leaves a product that absorbs only below 350 nm. The product spectrum in alkaline solutions, which is shown in Figure 4, undergoes further changes to species that absorb broadly in the near-UV and visible regions and are presumed to be ferric hydroxides. The intermediate product is not Fe(IV), since this species under similar solution conditions absorbs maximally at ≈420 nm.[12] It is most likely that this intermediate is a complex of iron(III) with hydrogen peroxide. An analogous species with similar spectral properties is $Fe^{III}ED$-$TA(O_2^{2-})$, which absorbs at 520 nm (ϵ = 530 M^{-1} cm^{-1})[20,21] and is unstable except in alkaline media. A visible absorption of $Fe^{III}(O_2^{2-}/^-O_2H)$ is not detectable during the oxidation of Fe-$(H_2O)_6^{2+}$ by O_2^- at pH 7[14] or after ferrate(V) decay, possibly because this transient dissociates on a much more rapid time scale than its formation.

The presence of hydrogen peroxide as a major product of ferrate(V) decay was confirmed by steady-state radiolysis. Solutions prepared under conditions nearly identical with those of pulse experiments were measured spectrophotometrically for loss of ferrate(VI) as a function of dose/time in the presence and absence of catalase. As shown in Figure 5, at irradiation times greater than 30 s all solutions exhibited a loss of ferrate(VI) in excess of that expected from the reaction with 2-propanol radicals (reaction 3). This must be attributed to slower reactions with products of ferrate(V) decay, since acetone and Fe^{III}–EDTA are unreactive. About 50% of this excess reducing power is eliminated by catalase and hence is due to hydrogen peroxide. Ferrate(VI)

(20) Walling, C. *Acc. Chem. Res.* **1975**, *8*, 125.
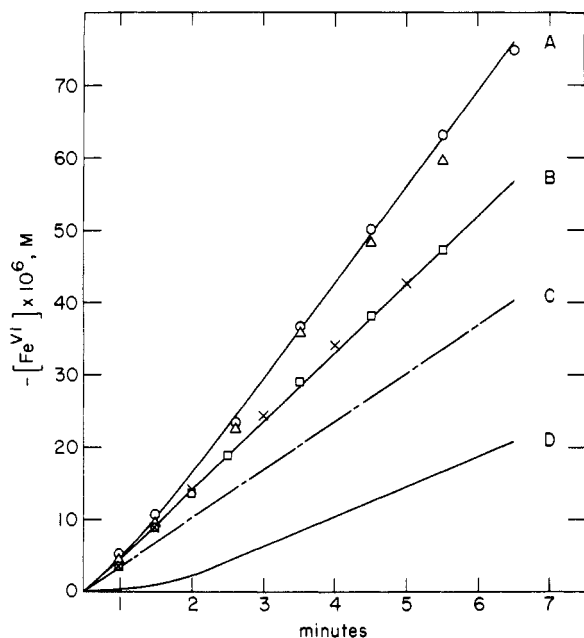(21) McClune, G. J.; Fee, J. A.; McClusky, G. A.; Groves, J. T. *J. Am. Chem. Soc.* **1977**, *99*, 5220.

Figure 5. Studies of the decrease in [Fe^{VI}] during steady-state radiolysis as a function of irradiation time. In addition to FeO$_4^{2-}$, all solutions contained 5 mM propanol, 0.026 M N$_2$O, and 2 mM phosphate/borate buffer at pH 10 and 25 °C. The four slopes shown represent the following: (A) (O) loss of Fe(VI) in absence of any other additives, ($\triangle$) loss of Fe(VI) in presence of 0.2 μM catalase; (B) ($\times$) loss of Fe(VI) in presence of 1.3 μM catalase, ($\square$) loss of Fe(VI) in presence of 2.6 μM catalase; (C) calculated slope assuming a loss of Fe(VI) with G[-Fe(VI)] = 6.1; (D) rate of disappearance of Fe(VI) in the presence and absence of catalase, i.e. slope (A) - slope (B).

oxidizes hydrogen peroxide to oxygen stochiometrically with a second-order rate constant of approximately 70 M^{-1} s^{-1}.[6] The difference between plots A and B in Figure 5 yields G(-Fe(VI)) = 4.0, which is due to peroxide, and hence G(H$_2$O$_2$) $\approx$ 6. If the molecular yield of H$_2$O$_2$ (G = 0.72) is subtracted, this leads to an amount of peroxide that is about 75% of the stoichiometric quantity expected from eq 8. A similar mode of decay was

$$\text{Fe}^V \rightarrow \text{Fe}^{III} + \text{H}_2\text{O}_2 \qquad (8)$$
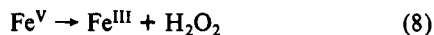
postulated in an earlier radiolysis study.[8] The excess of ferrate(VI) loss over that due to peroxide formation may arise from the reaction of some ferrate(V) with ferrate(VI) giving unknown products, or since peroxide is complexed with iron(III) as it is formed, we may expect competition between reaction 8 and the formation of iron(II) and superoxide (which is not scavenged by catalase), especially at alkaline pH. Carr et al.[7] have reported that ferroin is formed when ferrate(VI) decomposes in solutions containing o-phenanthroline, and it is likely in this case as well that the ferrous state is produced by the reduction of Fe(III) with hydrogen peroxide. The reaction between ferrate(V) and ferrate(VI) is relatively slow at pH 11.5 (k(Fe^V + Fe^{VI}) $\approx$ 5 $\times$ 10^3 M^{-1} s^{-1}) but could increase at a lower pH. Overall our treatment does not include potential reactions (e.g. Fe^V + H$_2$O$_2$, Fe^{II} + H$_2$O$_2$, etc.) and therefore the analysis for hydrogen peroxide is not to be considered quantitative but rather indicative that peroxide is a major product of Fe^V decomposition.

Discussion

As mentioned above, the products of unimolecular and bimolecular decay of ferrate(V) have the same absorption spectrum. Mechanistically, the bimolecular process could involve direct bond formation between oxide ligands. The remarkable feature of the ferrate(V) bimolecular decomposition is that a process involving the formation of covalent bonds occurs at rates typical of radical–radical interactions. The comparable observed second-order rate constants of ferrate(VI) decay are 4–5 orders of magnitude slower.

In the first transition-metal series, the oxo–metal bonds, which are necessary to stabilize valence states higher than IV, become

less common as the d orbitals are progressively occupied. The d^3 configuration of ferrate(V) is shared by manganese(IV)[22a] and chromium(III),[22b] the aqueous complexes of which are normally octahedral. However, of d^2 systems in the first transition-metal series, only ferrate(VI) and manganage(V)[22c] form tetrahedral oxoanion structures in solution. A conventional explanation, such as that given by Ochai,[23] is that progressive filling of the t$_2$ levels decreases the extent to which 2p electrons of oxygen can π-bond to these metal orbitals. As shown by Mössbauer spectroscopy,[5] the covalent FeO bonds in ferrate(VI) lend it a higher d-orbital electron density than would be expected from the formal configuration.

On the pulse-radiolysis time scale, the tetrahedral structure of the parent ferrate(VI) ion may be retained but is likely unstable with respect to higher coordination numbers. Vanadium(V), a d^0 system, is tetrahedral in alkali, but protonation favors the formation of six-coordinate species and aggregates.[22d] Since the ultimate product of ferrate(V) decay is iron(III) with possible iron(IV) intermediates, protonated forms of Fe(V) may have a lower activation barrier to the necessary rearrangement from four- to six-coordination. The second-order decay pathways involve mutual reduction rather than disproportionation. In Scheme I, it is being

Scheme I
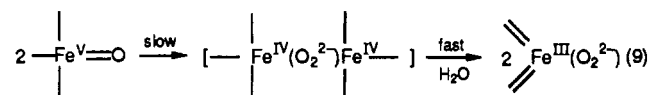
suggested that oxide ligands are oxidized to hydrogen peroxide in the rate-determining step followed by further fast oxidation/reduction steps, yielding two molecules of an iron(III) peroxo complex. Previous observations of the decay of iron(IV)[24] indicate that it decomposes by an analogous second-order pathway, but it was not observed as a free transient in iron(V) reduction. The direct formation of a peroxide bond by reaction between oxide ligands would be compatible with a substantial free-radical character of the ligand, which protonations may enhance by reducing resonance delocalization. An alternate mechanism involving the formation and rapid decay of an undetected diferrate(V) species would require that the rates of ligand substitution on ferrate(V) species be very much greater than the slow rate of oxygen exchange (2 $\times$ 10^{-3} s^{-1})[6] exhibited by FeO$_4^{2-}$. The correlation between solvent exchange processes and dimerization rates seems well established in the chromate/dichromate system.[25] We cannot exclude a rate-limiting step involving nucleophilic attack on the iron center, but the magnitude of k_1-k_4 seem too large for such a process unless the actual structure of ferrate(V) is distorted from tetrahedral. Although more information is needed to settle the structural aspects of FeO$_4^{3-}$, the observations made in this study appear to extend an earlier reported trend for MoO$_4^{2-}$ and WO$_4^{2-}$,[26] which has been recently corroborated by a pulse-radiolysis study of TcO$_4^{2-}$ and ReO$_4^{2-}$,[27] that tetrahedral oxoanions of the second and third transition rows are stable in alkaline solutions but convert to octahedral species in acid media. The observed enhancement of this conversion process upon descending from the second to the third transition series has been ascribed to the slight increase in size, which apparently allows a more easy expansion of the first coordination sphere. As suggested above, the reduction of ferrate(V) is likely to involve an activation barrier toward its rearrangement to an octahedral geometry. The first-order decay of FeO$_4^{2-}$ (k_f = 8.0 s^{-1}) to iron(III) and hydrogen peroxide seems to require that the coordination sphere of iron(V) expand prior to intramolecular oxidation/reduction. The oxidation

(22) (a) Cotton, F. A.; Wilkinson, G. *Advanced Inorganic Chemistry*, 5th ed.; Wiley & Sons: New York, 1988; pp 706–707. (b) *Ibid.*, pp 686–690. (c) *Ibid.*, p 707. (d) *Ibid.*, pp 668–671.
(23) Ochai, E. I. *Inorg. Nucl. Chem. Lett.* **1974**, *10*, 453.
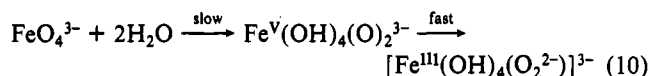(24) Melton, J. D.; Bielski, B. H. J. *Radiat. Phys. Chem.*, submitted for publication.
(25) Pladziewicz, J. R.; Espenson, J. E. *Inorg. Chem.* **1971**, *10*, 634.
(26) Honig, D. S.; Kustin, K. *Inorg. Chem.* **1972**, *11*, 65.
(27) Lisbon, K.; Sullivan, J. C.; Mulac, W. A.; Gordon, S.; Deutsch, E. *Inorg. Chem.* **1989**, *28*, 375.

of water, such as occurs slowly in alkaline permanganate solutions, may be disregarded, since in ethanolic media this would initiate the chain reduction of ferrate(VI) via OH and alcohol radicals, which is not observed during pulse-radiolysis experiments. In the more likely case that hydrogen peroxide is formed from oxide ligands of iron, the rate-limiting step would involve hydration of iron(V) followed by the reductive elimination of peroxide from cis oxide or hydroxide ligands as suggested in Scheme II.

Scheme II

$$FeO_4{}^{3-} + 2H_2O \xrightarrow{\text{slow}} Fe^V(OH)_4(O)_2{}^{3-} \xrightarrow{\text{fast}}$$
$$[Fe^{III}(OH)_4(O_2{}^{2-})]^{3-} \quad (10)$$

The degree of hydrolysis for an octahedral iron(V) species is unknown, but it is probably extensive for the high oxidation state in alkaline solution. Cis oxide ligands are found, for instance, in the pentavalent vanadium ion, $VO_2(H_2O)_4{}^{+}$.[22d] The product, ferric-bound peroxide, could form directly, without dissociation of an Fe^VO ligand bond, if the peroxide moiety is bound in a side-on mode as it is in the $Fe^{III}EDTA(O_2{}^{2-})^{3-}$ complex.[28]

The chemistry of iron(V) is virtually unknown, but the present study suggests that its stability may be enhanced in aprotic and weakly coordinating solvents where both of its known decay modes are likely to be inhibited. Efforts are currently in progress to prepare iron(V) under conditions that will permit more detailed studies of its properties.

(28) Ahmad, S.; McCallum, J. D.; Shiemke, A. K.; Appelman, E. H.; Loehr, T. M.; Sanders-Loehr, J. *Inorg. Chem.* **1988**, *27*, 2230.

Contribution from Ames Laboratory and the Department of Chemistry, Iowa State University, Ames, Iowa 50011

Effect of Steric Crowding on the Rates of Reactions of a Nickel(I) Tetraaza Macrocycle with Organic Halides and Hydroperoxides

Novelette Sadler,[1] Susannah L. Scott, Andreja Bakac,* James H. Espenson,* and M. S. Ram

The reactions of the sterically crowded decamethylcyclam complex of nickel(I), Ni(dmc)$^+$, with organic halides, hydrogen peroxide, and *tert*-butyl hydroperoxide occur some 10^4 times more slowly than the corresponding reactions of Ni(tmc)$^+$, a tetramethylcyclam complex. This supports the assignment of an inner-sphere mechanism in both cases, because reactions that necessarily adopt an outer-sphere mechanism (e.g., those of cobalt(III) amine complexes) differ no more in their relative rates than can easily be explained by the small difference in driving force.
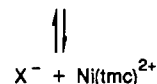
Introduction

Significant progress has been made in recent years in understanding the chemistry of macrocyclic complexes of Ni(II) and Ni(I). The most extensively studied of these complexes are those containing the 1,4,8,11-tetraazacyclotetradecane (cyclam) ligand as well as the N-alkylated and C-alkylated derivatives.[2-5] Among these are tetramethylated (tmc) and decamethylated (dmc) macrocycles.

It has been established that these Ni(II) macrocycles can be reduced electrochemically[6] or photochemically[7] to generate reasonably stable Ni(I) complexes in aqueous solutions. This provides the opportunity for investigations of the reduction of alkyl halides by Ni(I) to be carried out.

The oxidation of two isomeric forms of Ni(tetramethylcyclam)$^+$, abbreviated Ni(tmc)$^+$, by alkyl halides and hydroperoxides has been investigated recently.[7-12] The reactions were proposed to occur in two steps:

$$Ni(tmc)^+ + RX \xrightarrow{\text{rds}} Ni(tmc)^{2+} + X^- + R^\bullet \quad (1)$$

$$Ni(tmc)^+ + R^\bullet \rightarrow RNi(tmc)^+ \quad (2)$$
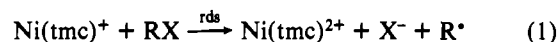
Electron transfer in the rate-determining step can occur by either an inner-sphere (eq 3) or an outer-sphere mechanism (eq 4).

$$Ni(tmc)^+ + RX \longrightarrow XNi(tmc)^+ + R^\bullet \quad (3)$$

$$\Updownarrow$$

$$X^- + Ni(tmc)^{2+}$$

$$Ni(tmc)^+ + RX \longrightarrow Ni(tmc)^{2+} + RX^{-\bullet} \quad (4)$$

$$\Updownarrow$$

$$X^- + R^\bullet$$

A distinction between the two mechanisms is a difficult one to make owing to the lability of Ni(tmc)$^{2+}$ to axial substitution. The reactivity pattern for a series of alkyl halides, i.e. CH_3 < primary < secondary < benzyl and Cl^- < Br^- < I^-, is similar to that observed in corresponding reactions of Co(II)[13] and Cr(II).[14] The latter reactions are known to proceed by an inner-sphere mechanism, and thus one might be tempted to conclude that the reactions of Ni(tmc)$^+$ adopt the same mechanism. This argument needs to be further substantiated by other evidence. It was against this background that we undertook the present study with the

(1) On leave from the Univesity of the West Indies, Kingston, Jamaica.
(2) Barefield, K. E.; Wagner, F. *Inorg. Chem.* **1973**, *12*, 2435.
(3) Wagner, F.; Barefield, K. E. *Inorg. Chem.* **1976**, *15*, 408.
(4) Wagner, F.; Mocella, M. T.; D'Aniello, M. J., Jr.; Wang, A. H. J.; Barefield, K. E. *J. Am. Chem. Soc.* **1974**, *96*, 2625.
(5) Lincoln, S. F.; Coates, J. H.; Hadi, D. A. *Inorg. Chim. Acta* **1984**, *81*, L9.
(6) Jubran, N.; Ginzberg, G.; Cohen, H.; Koresh, Y.; Meyerstein, D. *Inorg. Chem.* **1985**, *24*, 251.
(7) Bakac, A.; Espenson, J. H. *J. Am. Chem. Soc.* **1986**, *108*, 713.
(8) Bakac, A.; Espenson, J. H. *J. Am. Chem. Soc.* **1986**, *108*, 719.
(9) Bakac, A.; Espenson, J. H. *J. Am. Chem. Soc.* **1986**, *108*, 5353.
(10) Ram, M. S.; Bakac, A.; Espenson, J. H. *Inorg. Chem.* **1988**, *27*, 4231.
(11) Ram, M. S.; Bakac, A.; Espenson, J. H. *Inorg. Chem.* **1986**, *25*, 3267.
(12) Ram, M. S.; Bakac, A.; Espenson, J. H.; Bakac, A. *Inorg. Chem.* **1986**, *25*, 4115.

(13) Chock, P. B.; Halpern, J. *J. Am. Chem. Soc.* **1969**, *91*, 582 and references therein.
(14) Kochi, J. K. *Organometallic Mechanisms and Catalysis*; Academic Press: New York, 1978; p 140.